Magmatic compositions and source terranes estimated from melt inclusions in detrital Cr-rich spinels: An example from mid-Cretaceous sandstones in the eastern Tethys Himalaya

Bin Zhu*, John W. Delano, William S.F. Kidd

Department of Earth and Atmospheric Sciences, University at Albany, Albany, NY 12222, USA

Abstract

Cr-rich spinel is a detrital component within turbidites from the well-exposed, mid-Late Cretaceous Tianba Formation sequence in the Nieru Valley, southern Tibet. About 5% of the spinels contain melt inclusions, most of which are partly crystallized. To homogenize the crystallized melt inclusions for subsequent analysis by electron microprobe, spinels were heated at 1200 °C and 1250 °C for 96 h at controlled oxygen fugacity (FMQ) and quenched. This technique differs significantly from those previously applied by other investigators to melt inclusions in spinels, in having oxidation fugacity and temperatures more closely resembling natural conditions. The compositions of the melt inclusions correlate well with those of host spinels. The geochemistry of the melt inclusions and the Cr-rich spinels in the Tianba Formation turbidites suggests that the source of the Cr-rich spinels was hotspot basalts. Based on palaeo-tectonic reconstructions, presence of mid-Late Cretaceous fossils in the strata, and the chemical compositions of melt inclusions and detrital spinel, we infer that the volcanics of Rajmahal, which are associated spatially and temporally with Kerguelen hotspot activity on India about 117 Ma ago, were the likely source of these Cr-rich spinels.
© 2005 Elsevier B.V. All rights reserved.

Keywords: melt inclusions; detrital spinel; Himalaya; Rajmahal Basalts; mid-Cretaceous

1. Introduction

The chemical composition of erupted igneous rocks may be substantially different than the compo-

sition of the primary melts from which they were derived, to the point that many characteristics of the primary melt may be obscured by fractional crystallization, magma mixing, hydrothermal alteration, degassing, and assimilation of wall rocks [1]. Melt trapped in minerals during crystal growth provides information about the composition of the magma at the time of its effective isolation from the influence of

---

* Corresponding author. Tel.: +1 518 442 4466; fax: +1 518 442 5825.
E-mail address: zhub@atmos.albany.edu (B. Zhu).

subsequent fractionation processes [2–5]. Melt inclusions can reveal melt evolution that may not be recorded in bulk-rock data. Studies of melt inclusions in the earliest crystallized phenocrysts (e.g., olivine; Cr-rich spinel) therefore have provided constraints on the primary melt composition and evolutionary environments of parental magma [6–17]. Since Cr-rich spinels may be enriched in some sedimentary rocks due to their chemical durability against weathering, lack of cleavage, and resistance to low-grade alteration and mechanical breakdown [18–21], studies of Cr-rich spinels with melt inclusions in ancient
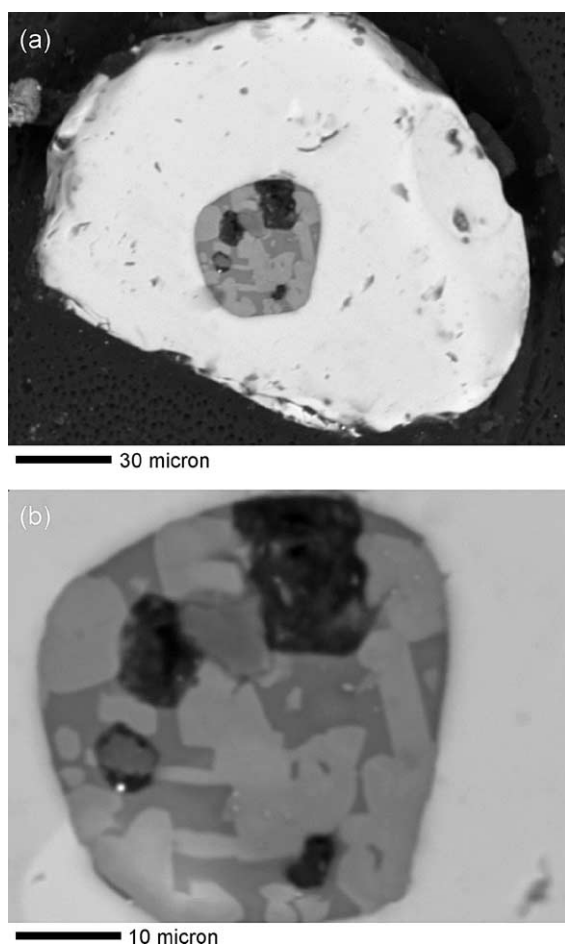

Fig. 1. Backscattered electron images of (a) a partly crystallized melt inclusion in a detrital spinel grain from the Tianba Formation (scale bar=30 μm); (b) enlargement of the melt inclusion (scale bar=10 μm) consisting of pyroxene crystals (light grey), residual glass (dark grey), voids (black), and minor sulfide droplet (bright spot). Broad beam analysis (1) is shown in Table 1.

sediments have the potential to give information on provenance and tectonic evolution in a complex orogenic system [8,22].

We report chemical compositions of melt inclusions (Fig. 1) trapped in Cr-rich spinels from the Cretaceous Tianba Formation at the north end of Nieru Valley (N28° 44′, E89°57′), southern Tibet (Fig. 2), that provide compositional constraints on the tectonic setting of the original source terrane for these spinels, thereby strengthening provenance studies of the sedimentary petrology based on detrital modal analyses of the sandstones. This is the first study of melt inclusions in detrital spinels in the Himalaya, the product of continent–continent collision between Asia and India.

2. Geologic setting

The Tethyan Himalaya, which are located between the High Himalayan Crystalline belt to the south and the Indus–Yarlung–Tsangpo Suture and the Lhasa block to the north (Fig. 2), consist primarily of late Paleozoic to early Eocene sedimentary rocks originally deposited along the northern edge of the Indian continent. Deposition began with late Paleozoic–Triassic rifting [23–25] during the initial development of the Neo-Tethyan Ocean. A wide passive continental margin subsequently developed along the north rim of the Indian continent. During the mid-Cretaceous, northward-directed subduction of the Neo-Tethyan oceanic crust beneath the southern margin of Asia resulted in the development of a magmatic arc and a forearc-related basin (Xigaze Forearc Basin) along the southern margin of the Lhasa block [26,27]. With continued subduction, the India–Asia collision initiated in the early Tertiary, which gave rise to the Indus–Yarlung–Tsangpo suture (IYZS). The strata of the Tethyan Himalaya record the entire depositional history of the northern Indian passive margin.

In southern Tibet, the Tethyan Himalaya are divided into two subzones of different lithological assemblages (Fig. 2) separated by the east–west trending Gyirong–Kangmar thrust [28]. The northern zone is dominated by slightly metamorphosed deposits of outer shelf, and continental slope and rise, while the southern zone is characterized by unmetamor-
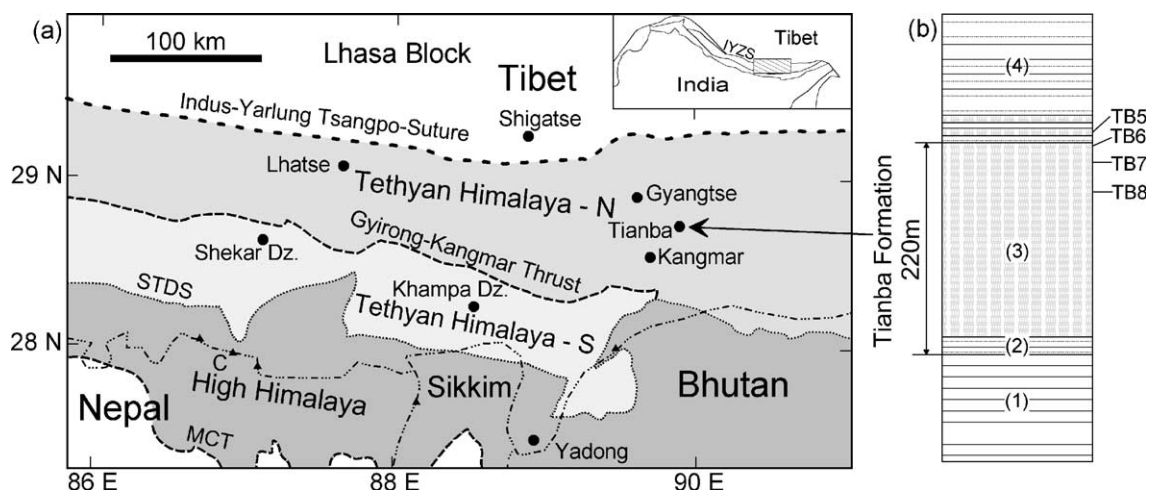
Fig. 2. (a) Simplified tectonic map of the east-central Tethyan Himalaya (after [33]). The inset map shows the position of this area in the Himalayan system. MCT—Main Central Thrust; STDS—southern Tibet detachment system; C—Cholmolungma. (b) Simplified stratigraphic column of the Tianba section (N28°44′, E89°57′): TB5–TB8 are four samples containing spinel. (1) Cherts and mudstones; (2) mica-rich siltstones; (3) sandstones/siltstones; (4) shales/minor sideritic sandstones. For the detailed stratigraphy, see [29].

phosed, shallow water shelf carbonate and terrigenous deposits ranging from late Paleozoic to Eocene in age.

This study concentrates on the well-exposed section of Cretaceous lithic arenites at the northern end of the Nieru Valley, which belongs to the northern zone of the Tethyan Himalaya. This lithologic unit, which we term the Tianba Formation (Tianba Flysch [29]), is an approximately 220-m-thick turbidite sequence and consists primarily of well-bedded sandstones with less abundant siltstones and shales. The contact between the Tianba Formation and the underlying dark shales and cherts is conformable. The basal interval of the Formation is characterized by the abrupt disappearance of black cherts and appearance of olive-colored argillites and mica-rich siltstones that coarsen up rapidly into medium to thick-bedded (>1 m) graded sandstones. Individual sandstone beds are normally graded into siltstones and shales, and contain abundant sedimentary structures ordered in a Bouma sequence, indicating a "proximal" turbidite fan depositional environment for the Tianba Formation. There is no evidence for storm wave influence in this stratigraphic unit (reworked bed tops, hummocky cross-bedding, etc.), nor in those above and below it; and we reject the idea that they might be "outer shelf" deposits.

The top of the Tianba Formation is characterized by a sharp termination of the turbiditic sandstones,

which are conformably overlain by greenish–grey burrowed shales. These shales also contain a few thin sideritic sandstone beds in the first 10–15 m, and some large (up to 1 m in diameter) calcareous nodules in the interval ~60–70 m above the Formation. One of the nodules yielded an ammonite, and some belemnites are found in the shales above the Formation. Preliminary investigation of radiolarian fossils in the sideritic sandstones indicates deposition sometime within the mid-Late Cretaceous (N. Shafique, personal communication, 2002). There are abundant pelagic fossils (ammonites, belemnites, and bivalves) of Valanginian–Aptian age (141–125 Ma) in the shales that conformably underlie the Tianba Formation [30–33]. Consequently, all the evidence suggests that the Tianba Formation was deposited during mid Cretaceous time in a deep-water setting (continental rise, or lower slope) of the outer Indian passive margin.

3. Sandstone petrography and framework modes

Sandstones of the Tianba Formation are lithic wackes characterized by poorly sorted, subangular quartz with significant lithic content, and generally abundant matrix (10–30%). Quartz is dominant (average=62%), and commonly has inclusions of

feldspar, biotite and zircon. Feldspar comprises 1–6% of the total grain population. Sedimentary rock fragments (siltstone, shales, micritic limestones) are often present (2–3%) in medium and coarser sandstones, as well as metamorphic grains (1–4%). Volcanic clasts (2–5%) contained in the wackes are both mafic and silicic in composition, which suggest derivation from a terrane containing significant volcanic areas.

Samples were crushed, sieved, and the 90–250-μm fraction separated in the heavy liquid tribromomethane (density 2.89 g/cm^3) to extract the heavy minerals from the Tianba Formation. The heavy mineral suite consists of a low-diversity, zircon-rich assemblage with varying amounts of tourmaline, apatite, rutile, magnetite, pyrite, and Cr-rich spinel. The significant volcanic component of Tianba Formation is reflected by the abundance of sharp euhedral, elongate, colorless zircons in the upper part of the unit. Four samples (Fig. 2b) from the upper sandstones of Tianba Formation and the sideritic sandstones were found to contain Cr-rich spinel, indicating a significant ultramafic and/or mafic magmatic source terrane.

4. Sample preparation and analytical methods

Cr-rich spinels dominate the heavy mineral population from the sideritic sandstones; some of these contain melt inclusions. To obtain the original composition of partially crystallized melt inclusions, high-temperature experiments on 400 spinel grains were performed with a 1-atm, gas mixing (CO+CO$_2$) Deltech furnace. The sample container was a Pt-foil basket that was suspended on a Pt-wire in the center of the furnace with a layer 2 mm thick of mantle olivine (~Fo92) powder to minimize Fe-loss from the Cr-rich spinels by being in contact with the Pt-foil. The oxygen fugacity was controlled at the fayalite+magnetite+quartz (FMQ) buffer by CO+CO$_2$ gas flow during heating. Following the studies of Roeder and Reynolds [34], spinels were heated in two separate experiments at 1200 °C and 1250 °C for 96 h to approach equilibrium between spinel and melt, and to homogenize the melt inclusions (Fig. 3a,b). Each experiment was terminated by electrically cutting the Pt-wire causing the sample to fall into water, with a quenching time of <1 s. The sample was kept at the

FMQ buffer up to the instant of quenching. These spinels were individually mounted in epoxy resin, polished and analyzed by electron microprobe. Only 19 out of 400 (~5%) of the heated Cr-spinel grains were found upon polishing to contain melt inclusions, and of these only 12 contained inclusions large enough to yield analyses with good totals.

Our homogenization method differed from some other approaches [8,13,15–17] in two important characteristics. First, instead of heating the minerals and inclusions for short times (~15 min) at high temperatures (1350–1400 °C), our experiments were performed for 96 h at temperatures of 1200 °C and 1250 °C. Second, instead of surrounding the inclusion-bearing crystals in an inert gas (e.g., He, Ar) during heating, our crystals were held at a constant and controlled oxidation state at the FMQ buffer. Our experiments also involved rapid (<1 s) quenching of the samples at the end of our experiments that yielded chemically homogeneous glass, instead of the comparatively slow cooling that would have allowed formation of minute crystallites.

The experimental conditions used during our homogenization experiments were designed to more closely simulate natural conditions in a magmatic system during the entrapment and partial crystallization of these melts. Terrestrial basaltic systems typically occur at temperatures in the range of 1050°–1150 °C, which are closer to our experimental temperatures than some previous studies (e.g., [8,13,15–17]). Since melt inclusions and their host mineral phases chemically interact in the natural post-entrapment environment, our experiments allowed for some partial re-equilibration between the host spinel and the melt inclusion, whereas other experimental approaches (e.g., [8,13,15–17]) assume that the melt inclusions had been chemically inert with respect to their host-mineral in the post-entrapment environment. A similar experimental approach to that used in the present study was employed by Gaetani and Watson [35] in their study of melt inclusions in olivine.

While enclosing inclusion-bearing crystals in a volume that has been purged with commercially available inert gas is a better environment than air for heating, it is still more oxidizing an environment than natural magmatic systems. For example, our measurements of the oxygen fugacity using a yttria-
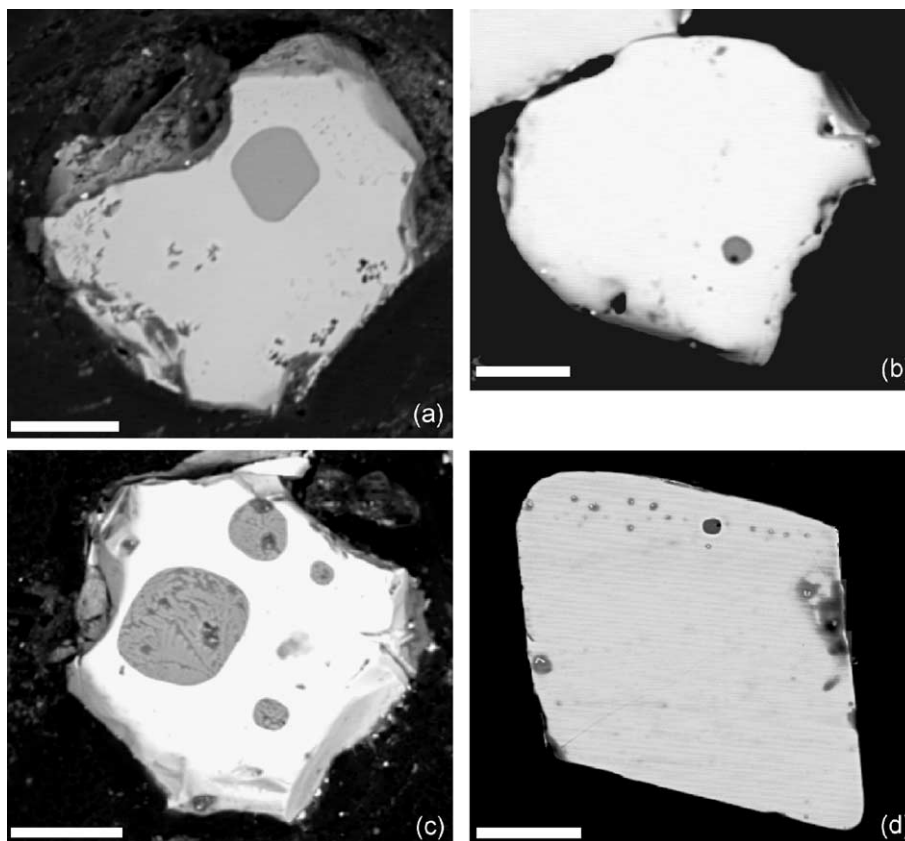
Fig. 3. Backscattered electron images of melt inclusions (darker grey) in Cr spinels from Tianba Formation (scale bars=30 μm). (a) Homogenized melt inclusion heated 96 h at 1250 C, analysis 11 in Table 1. (b) Homogenized melt inclusion heated 96 h at 1200 C, analysis 9 in Table 1. (c) Melt inclusions randomly distributed in a Cr-rich spinel (not experimentally heated), analysis 5 in Table 1. (d) Numerous small melt inclusions form a band parallel with the outline of an euhedral Cr-rich spinel.

doped zirconia sensor with commercially available Ar flowing through the furnace tube at 1200–1300 °C is about 10^{-3} bar O_2 (i.e., highly oxidizing) due to the presence of molecular oxygen as an impurity in the commercial product. In contrast, the oxygen fugacities during our experiments were at $10^{-8.5}$ bar (at 1200 °C) and $10^{-7.9}$ bar (at 1250 °C), both of which are known to be realistic values for terrestrial magmatic systems. Since our gas-mixing experiments were able to maintain these conditions (precisions: ± 2 °C; ± 0.05 log-units $f\,O_2$) throughout the duration of the heating, equilibrium partitioning between the enclosed melt and the host crystal could be approached, which is presumably closer to the natural conditions under which the melt inclusions were originally incorporated in the magmatic system. However, we do not know the actual temperatures

when these melt inclusions became trapped (i.e., isolated from the magmatic system). We selected 1200 °C and 1250 °C as temperatures that were (a) more realistic than some previously published studies that homogenized partially/completely crystallized melt inclusions, and (b) that would likely produce homogeneous, crystal-free melt inclusions within practical run-times under controlled redox conditions.

All microprobe analyses were performed using a JEOL 733 Superprobe (fully automated, five wavelength dispersive spectrometers) in the Department of Earth and Environmental Sciences at Rensselaer Polytechnic Institute. Standard procedures (accelerating voltage 15 keV, a beam current 15 nA, and a beam diameter of ≤ 5 μm, using ZAF correction model) were used to analyze the spinels with natural minerals and glasses as standards. Melt inclusions were analyzed

for the elements Si, Ti, Al, Ca, Fe, Mg, Mn, Na, K, and P; five X-ray spectrometers were tuned and calibrated for each element. Thirty-second counting time was used. The VG-2 basaltic glass standard was analyzed at intervals throughout the probing session to ensure that calibration did not drift. Na_2O was analyzed first in order to minimize the possible effect of Na loss during analyses. Backgrounds were collected for each element on each analysis. Relative errors were generally less than 1% of the amount present for major elements (Si, Fe, Al, Mg, Ca), and less than 5% of the amount present for minor elements (Ti, Na, K, P), except for Mn (15%).

5. Cr-rich spinel

The detrital spinels in grain mounts (Fig. 1) are in the 100- to 200-μm size range. They are dark brown to dark reddish–brown in thin section, a typical color for Cr-rich spinel [20]. While the spinel grains are opaque in visible light, some grains are weakly translucent at the edges. Grain margins commonly show conchoidal fractures, suggestive of mechanical breakage, but some grains are subhedral to euhedral.

Due to this mineral being opaque, melt inclusions were found by meticulously grinding down into the spinels, polishing, looking in a reflected light microscope, and repeating the process if no melt inclusion was found on that polished surface. This continued until a melt inclusion was found, or the spinel was ground away.

The microprobe results indicate that the compositions of the detrital Cr-rich spinels from Tianba Formation contain 15–26 wt.% Al_2O_3, 36–45 wt.% Cr_2O_3, 10–12 wt.% MgO, 20–30 wt.% FeO_t, and 1.5–2.0 wt.% TiO_2, typical for those of spinel from Hawaiian basalts [12,36–38]. There is an inverse relationship between Cr and Al, which may be indicative of different degrees of partial melting in the mantle [36]. MnO, NiO, V_2O_5, and ZnO are present in low abundances (generally <0.5 wt.%). Spinel grains showed no detectable zoning in line scans, which may indicate that most of the parental lava had undergone little or no magma mixing or significant crustal assimilation [39]. The relatively narrow range of chemical composition of these detrital spinels appears to exclude the possibility of a volcanic arc source because a wide variation in the chemical compositions are observed in spinels
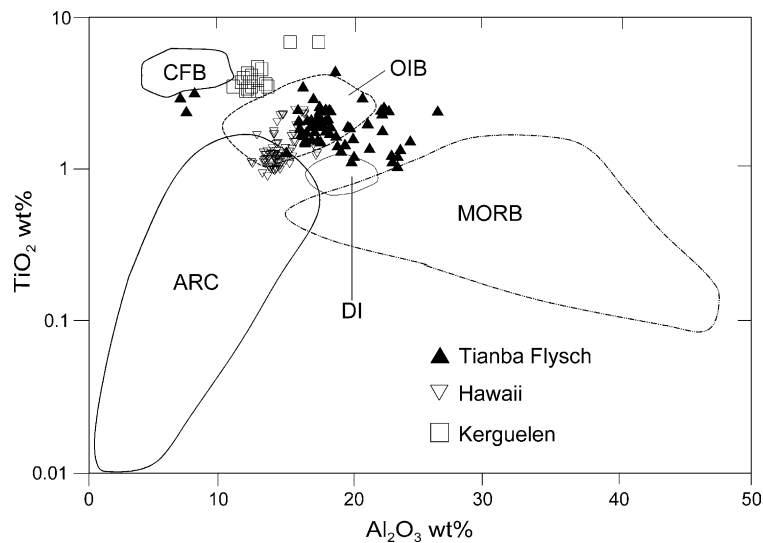

Fig. 4. Major element compositions of spinels on tectonic setting discriminant plot of TiO_2 vs. Al_2O_3 (after [12]). Studies of Cr-rich spinel compositions from different tectonic settings show that TiO_2 and Al_2O_3 contents of spinel form a linear trend for those from Continental Flood Basalts (CFB), Ocean Island Basalts (OIB), Disko Island, West Greenland (DI), and Mid-Ocean Ridge Basalts (MORB). Spinels from Hawaii are from Delano [unpublished data], and spinels from Kerguelen are from [41]. Our data [29] plot in the middle of this trend, mainly in the OIB field.

derived from arc complexes and associated accretionary complexes [37].

In a spinel discriminant plot (Fig. 4) the detrital spinels from Tianba Formation consistently plot in, or close to, the ocean island basalt (OIB) field. In agreement with this inference, these detrital spinels plot within the 'intra-plate basalts' field on a $Cr/(Cr+Al)$ versus TiO_2 discriminant diagram (not shown) of Lee [40]. Also shown in Fig. 4 are compositions of spinel inclusions in olivine from Hawaii (Delano, unpublished data), and Cr-rich spinels in Kerguelen plume-derived basalt [41]. The fact that most Tianba spinels plot in the OIB field (Fig. 4) suggests that the Tianba Formation detrital spinels were derived from hotspot-related volcanic rocks.

6. Melt inclusions

About 5% of the Cr-rich spinels were found to contain melt inclusions (Fig. 1) in the 5- to 60-μm size range. Some spinels contain multiple melt inclusions (Fig. 3c,d). Most of the melt inclusions are sub-euhedral to sub-round, and they align with the host spinel crystallographic direction (Fig. 3d). These features, which allow them to be identified as primary inclusions, are common for melt inclusions trapped during the crystallization of Cr-rich spinel [3]. Most melt inclusions are partially crystallized, and composed of pyroxene crystals, residual glass, and minor sulfide droplets. The presence of well-crystallized pyroxene (Fig. 1) suggests a relatively long cooling history and post-entrapment elemental exchange between the melt and the host spinel. The four pyroxene crystals in this inclusion (Fig. 1) have different abundances of the major-element oxides, as expected from closed-system crystallization at a cooling rate too rapid for subsolidus homogenization. This is consistent with the interpretation that the pyroxenes are not xenocrysts but true daughter crystals after entrapment of the melt in the spinel. A line scan on one unheated spinel with a melt inclusion shows that there is a significant composition change of the spinel over an interval of ~10 μm at the melt/spinel interface where Al_2O_3 increases from 18.0% to 29.2%, while Cr_2O_3 decreases from 36.2% to 26.1%. This is probably due to crystallization of Cr-rich

spinel along the inclusion walls after entrapment of melt [17].

Representative major-element compositions of the melt inclusions and host Cr-rich spinels are given in Table 1 and illustrated in Fig. 5. For comparison, unheated melt inclusions (i.e., crystal-bearing inclusions) were probed using broad beam analyses (a beam diameter of 10 μm). Among the experimentally heated inclusions, there is no correlation between the experimental temperature and melt inclusion compositions, except for MgO. Melt produced in the 1250 °C experiments had higher MgO abundances (>8%) than melts generated in the 1200 °C experiments (<8%). Because the unheated inclusions have a compositional spread in MgO comparable to both the 1200 °C and 1250 °C heated results together and no other elemental abundances are found to be correlated with the experimental temperatures, we think this apparent change in MgO composition with temperature is unlikely to be due to the temperature differences between the experiments. The fact that all host spinel grains heated at 1250 °C have higher abundances of MgO compared to most grains heated at 1200 °C (Fig. 6) may explain the high MgO in the "heated 1250 °C" melt inclusions. This issue requires further studies given the small data set we are able to report in this paper.

Compositions of melt inclusions (Table 1) are 42–52 wt.% SiO_2, 1.5–4.0 wt.% TiO_2, 10.2–18.0 wt.% Al_2O_3, 4.66–12.46 wt.% MgO, 9.01–16.67 wt.% CaO, 0.21–4.07 wt.% Na_2O, 0.1–1.6 wt.% K_2O, and 0.6–1.6 CaO/Al_2O_3. The Na_2O content in five analyses is <1%. To see if these low abundances were caused by Na mobility under the electron beam, some glass analyses using a lower current and a defocused beam were performed, but similar values were obtained in three separate probe sessions. Therefore we consider these analyses to be accurate. Thirteen analyses with Na_2O >1.5 wt.% suggest that the parental magmas for these samples were alkali rich, which is also consistent with the relative enrichments of incompatible elements (e.g., Ti, P, K) in the glass analyses (Table 1); the five analyses with Na_2O <1.5 wt.% suggest that some spinels came from tholeiitic basalts. The alkali–silica diagram [42] also shows that these melt inclusions were mostly from alkali basalts with a less abundant tholeiitic source (Fig. 7).

Table 1
Microprobe analyses of melt inclusions and host spinel from the Tianba Formation

	Unheat	Unheat	Unheat	Unheat	Unheat	Unheat	1200	1200	1200	1200	1250	1250	1250	1250	1250	1250	1250	1250
Glass	1	2	3	4	5	6	7	8	9	10	11	12	13	14	15	16	17	18
SiO_2	52.25	49.39	52.05	46.69	47.86	41.79	46.14	46.71	45.91	45.19	44.17	51.19	42.75	46.18	47.96	45.51	41.50	43.72
TiO_2	1.85	1.54	1.50	1.79	1.79	2.88	4.02	2.12	1.78	3.98	3.19	1.98	1.68	1.78	1.71	1.93	1.82	3.17
Al_2O_3	11.03	13.85	14.56	14.86	14.79	17.98	15.76	15.38	13.31	15.18	13.86	13.67	15.19	12.38	10.19	15.00	11.54	13.67
Cr_2O_3	0.67	0.64	1.22	1.03	1.01	5.20	1.06	1.40	1.27	1.02	0.87	1.10	1.22	1.60	0.91	1.40	1.31	0.83
FeO	4.01	10.67	10.39	9.35	9.71	10.59	5.43	9.06	12.22	5.69	12.06	9.09	11.31	13.10	10.16	12.18	13.55	12.08
MnO	0.09	0.16	0.21	0.16	0.14	0.09	0.11	0.13	0.18	0.10	0.22	0.20	0.18	0.22	0.13	0.14	0.22	0.20
MgO	11.00	8.34	6.74	6.18	6.28	6.79	6.12	4.66	7.72	5.89	8.89	12.46	10.94	10.77	10.24	10.68	9.79	8.78
CaO	14.21	12.90	10.91	12.00	11.74	10.32	13.93	11.55	11.85	13.84	11.89	8.96	12.38	12.33	16.67	13.10	11.66	11.78
Na_2O	0.78	0.45	0.55	2.96	2.17	1.69	3.27	3.24	2.37	4.07	2.33	0.41	2.22	2.34	0.21	2.72	2.26	2.11
K_2O	0.82	0.50	0.29	0.93	0.84	0.60	0.76	1.64	0.66	0.73	1.14	0.14	0.60	0.67	0.09	0.56	0.70	1.17
P_2O_5	0.44	0.31	0.36	0.34	0.36	0.35	0.51	0.24	0.26	0.52	0.62	0.04	0.20	0.24	0.23	0.20	0.34	0.69
Total	97.16	98.76	98.78	96.30	96.68	98.28	97.22	96.26	97.54	96.22	99.23	99.22	98.67	101.59	98.71	103.41	94.70	98.20
CaO/Al_2O_3	1.29	0.93	0.75	0.81	0.79	0.57	0.88	0.75	0.89	0.91	0.86	0.66	0.82	1.00	1.64	0.87	1.01	0.86
Na_2O+K_2O	1.60	0.95	0.84	3.88	3.01	2.29	4.03	4.88	3.04	4.80	3.47	0.54	2.82	3.01	1.28	3.28	2.96	3.28
Spinel																		
Al_2O_3	21.17	17.31	17.33	17.77	17.77	7.45	18.5	18.38	16.86	16.04	21.7	17.53	16.85	18.17	16.84	17.68	21.2	22.37
TiO_2	1.93	2.75	1.38	1.90	1.74	2.45	2.75	1.71	2.06	2.72	2.56	1.62	1.66	1.64	1.57	1.96	1.62	2.53
MgO	11.17	12.48	12.48	9.53	10.39	9.55	12.12	10.65	10.72	9.57	12.57	13.52	12.97	12.48	12.85	12.56	12.74	13.51
MnO	0.27	0.24	0.28	0.29	0.21	0.32	0.20	0.32	0.25	0.27	0.25	0.21	0.20	0.26	0.24	0.27	0.29	0.29
FeO	16.62	15.69	14.09	17.72	16.95	17.95	16.20	17.26	16.73	19.15	15.49	13.00	13.38	14.55	13.73	14.40	14.61	14.31
Fe_2O_3	10.99	10.30	12.57	13.09	13.96	10.26	9.08	10.42	13.21	8.80	12.97	11.55	12.02	11.85	15.70	11.50	11.66	11.67
NiO	0.25	0.16	0.19	0.15	0.12	0.18	0.05	0.24	0.18	0.12	0.27	0.14	0.18	0.17	0.18	0.24	0.23	0.21
V_2O_5	0.12	0.38	0.32	0.19	0.19	n.a.	n.a.	0.26	0.19	n.a.	0.20	0.22	0.19	0.37	n.a.	0.22	0.32	n.a.
Cr_2O_3	36.35	41.14	41.25	36.26	37.38	52.53	40.68	40.86	38.98	41.93	34.15	42.07	41.61	40.43	39.89	40.77	37.58	35.41
Total	98.86	100.45	99.89	96.91	98.70	100.69	99.59	100.10	99.19	98.60	100.15	99.87	99.05	99.93	101.01	99.61	100.25	100.30
Mg/(Mg+Fe2+)	0.49	0.53	0.54	0.43	0.46	0.44	0.52	0.47	0.47	0.43	0.52	0.58	0.57	0.54	0.55	0.54	0.54	0.56
Cr/(Cr+Al)	0.54	0.61	0.61	0.58	0.59	0.83	0.60	0.60	0.61	0.64	0.51	0.62	0.62	0.60	0.61	0.61	0.54	0.51

The ferric iron content for spinel was determined by assuming stoichiometry ([37]).
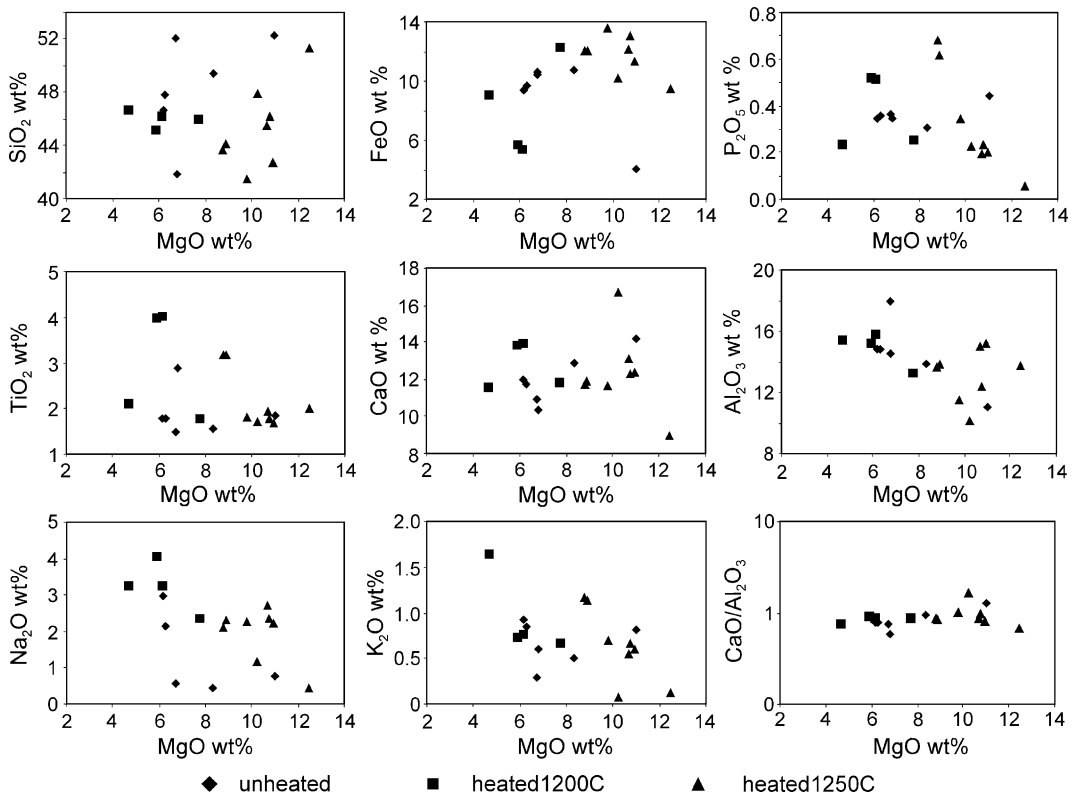n.a.—Not analyzed.

Fig. 5. Major-element compositions of melt inclusions in the detrital spinels from Tianba Formation.
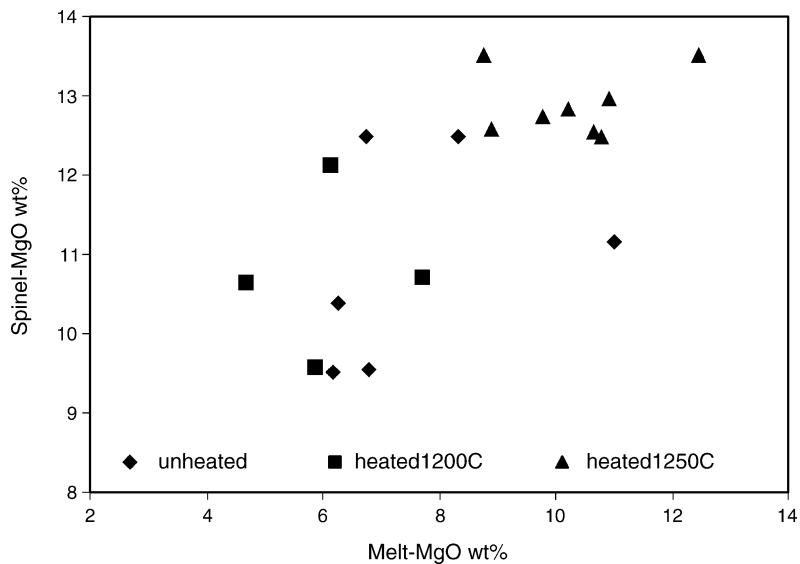

Fig. 6. Relationship between host spinel and melt inclusion MgO contents.
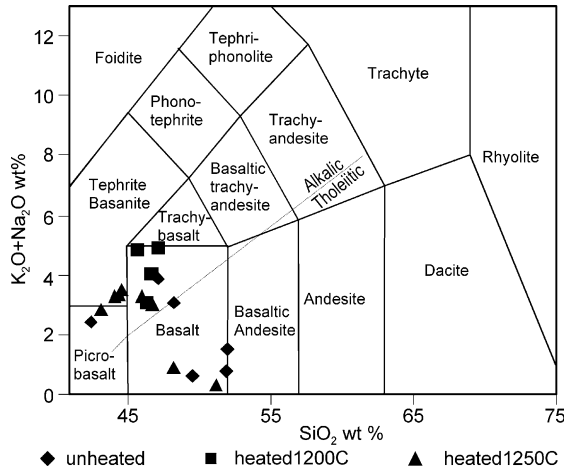
Fig. 7. Total alkalis versus silica plot after [42]. In our glass data, there are 13 analyses with Na_2O content >1.5 wt.%, and 5 are <1.5%, forming two populations of melt compositions, one of alkali and one of tholeiitic basalts.

The Cr_2O_3 abundances measured by electron microprobe in melt inclusions (0.6–5.2%) are significantly higher than that in typical basalts [43]. Roeder and Reynolds [34] demonstrated that Cr solubility in basaltic melts increases with increasing temperature and decreasing oxygen fugacity, and that spinels containing 30–50 wt.% Cr_2O_3 are in equilibrium with terrestrial basaltic melts having 0.02–0.06 wt.% Cr_2O_3 at the oxygen fugacity of ~FMQ. Consequently, the measured Cr_2O_3 abundances of ~1 wt.% in these melt inclusions (Table 1) are not likely to be real. In agreement with Sigurdsson et al. [17] and Roeder and Reynolds [34], we attribute the high Cr_2O_3 abundances to either secondary fluorescence and/or beam overlap from the host Cr-rich spinel (i.e., analytical artifact). The implications of this for estimating the actual compositions of melts associated with their host Cr-rich spinels are illustrated by tie-lines in Fig. 8 that connect melt+spinel pairs and project back toward the original melt composition [44]. If our suggestion of an
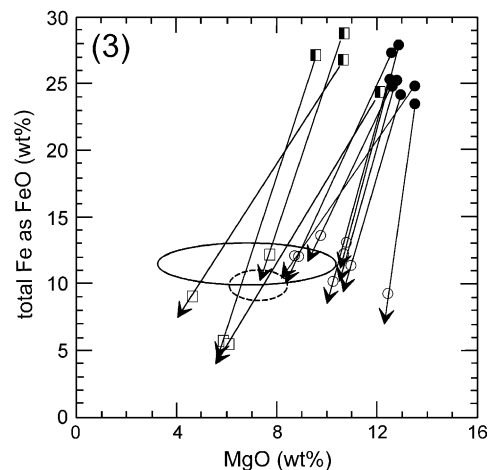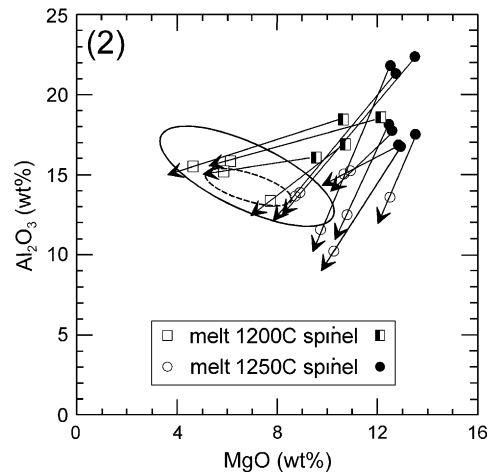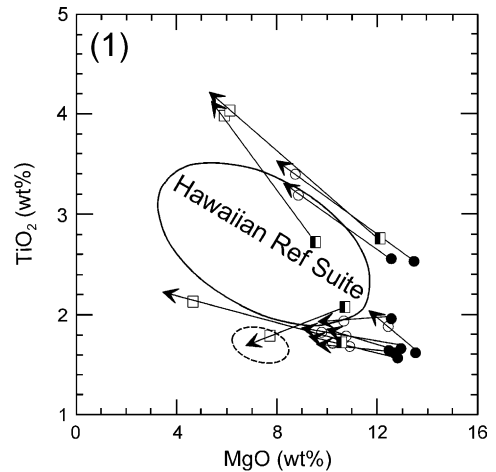
Fig. 8. Spinel-melt compositional pairs to extract original melt composition. Tie-lines connecting spinel and melt compositions from the 1200 °C and 1250 °C experiments are shown. Since the melts may have dissolved some of the host spinel during the experiments, the tie-lines project in the direction of the original melt compositions. The dashed ellipse in each figure is the location of the unheated inclusions (for reference). The Hawaiian Reference Suite (in solid elliptical field) is from [45].

analytical artifact is correct, the melt analyses in Table 1 may be treated as 0.970–0.975 fraction of the actual melt and 0.025–0.030 fraction of host spinel. The compositions of the actual melts would differ from the analyses in Table 1 in the following ways: lower in MgO by ~0.2 wt.%; higher in SiO_2 by ~1.0 wt.%; higher in TiO_2 by ≤0.1 wt.%; lower in Al_2O_3 by ~0.2 wt.%; lower in total Fe as FeO by ~0.5 wt.%; higher in CaO by ~0.4 wt.%; higher in Na_2O by ~0.1 wt.%.

Kamenetsky et al. [12] observed a strong correlation for TiO_2 between melt inclusions and hosted spinel for a range of magma types and tectonic settings (Fig. 9), indicating that their abundances in spinels are primarily dependent on the magmatic TiO_2. Similarly, our data, which plot near the OIB

Fig. 10. Discriminant function plot of basalts from three tectonic settings. The compositions of basalt (SiO_2:40–55 wt.%) from Arc, MORB, and hotspot-related basalts [43,45] were used to develop this plot using linear discriminant function in the Splus software package. The boundaries of the fields shown are 95% confidence lines.

$$D1 = 2.02*\log(SiO_2/TiO_2) - 2.15*\log(Al_2O_3/TiO_2)$$
$$- 0.14*\log(FeO/TiO_2) + 0.82*\log(CaO/TiO_2)$$
$$+ 0.41*\log(MgO/TiO_2) - 1.07*\log(K_2O/TiO_2)$$
$$- 0.37*\log(Na_2O/TiO_2) + 0.53*\log(P_2O_5/TiO_2)$$

$$D2 = 1.69*\log(SiO_2/TiO_2) - 2.88*\log(Al_2O_3/TiO_2)$$
$$- 0.09*\log(FeO/TiO_2) + 0.85*\log(CaO/TiO_2)$$
$$- 0.49*\log(MgO/TiO_2) - 1.15*\log(K_2O/TiO_2)$$
$$+ 3.48*\log(Na_2O/TiO_2) - 0.17*\log(P_2O_5/TiO_2)$$

Note: Due to the constant sum problem for compositional data, we follow the method of Aitchison [46] to use log ratios as a data matrix in linear discriminant function analysis (lda), which is a classical statistical approach for classifying samples of unknown classes, based on training samples with known classes. The lda function in Splus generates the formula above.

Fig. 9. TiO_2 contents in melt inclusions and host spinels. Data of this study shown with fields drawn from compositional averages of Kamentsky et al. ([12]). Enlargement of the upper right portion of the full plot is shown above.

field, show a positive correlation. Our data show no evidence for Cr-rich spinels in the Tianba Formation having been derived from arc complexes (Fig. 9).

We have developed a discriminant plot (Fig. 10) to separate basaltic rocks from hotspot, MORB and arc assemblages, based on major oxide compositions of 600 basalts [43,45] from well-studied areas. Eleven of 18 analyzed melt inclusions in spinel from Tianba Formation plot in the hotspot field for this plot, and there are no points in the arc field. There is a significant overlap between the observed compositions of the melt inclusions and published Rajmahal basalt compositions [47,48].
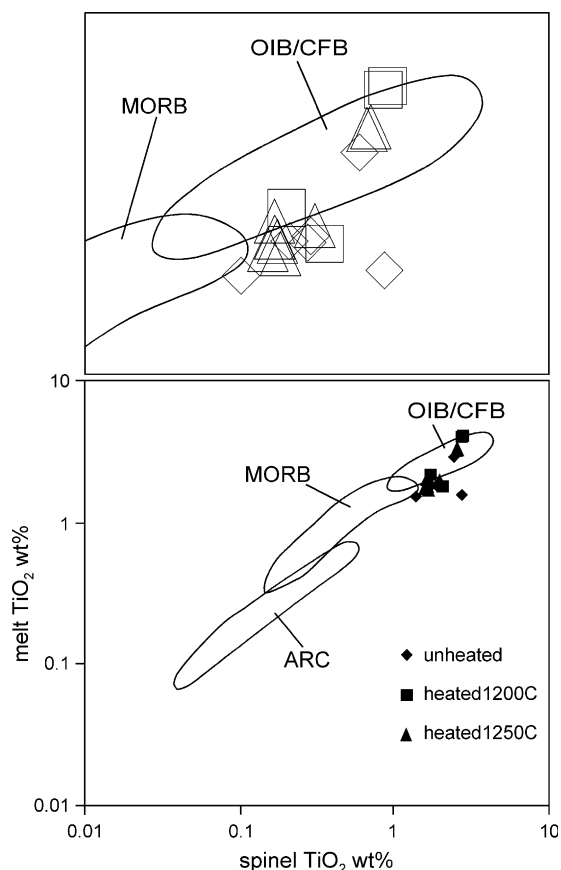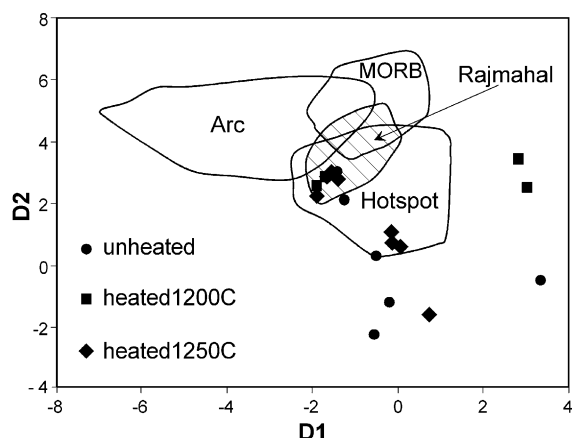
7. Discussion

7.1. Heating time of homogenization experiment

A key question in this study is whether the re-homogenized melt inclusions represent the composition of the parental magma. Most workers heat crystal-bearing inclusions in Cr-rich spinel for only 10 to 30 min in an attempt to limit re-equilibration between the melt inclusions and spinel, and/or in situ crystallization of spinel [8,15,17].

Danyushevsky et al. [10] argued that during homogenization experiments, the phenocrysts may control the compositions of melt inclusions due to their dominant size, and that the composition of a melt is a function of the physical conditions of the experiment and the phenocryst composition when chemical equilibrium is established. In contrast, during crystallization in natural magma systems, the melt composition controls the composition of crystallizing phases, i.e., the composition of a phenocryst is a function of the physical conditions and melt composition. Therefore they suggested that the melt inclusions should be kept at high temperatures (~1300 °C) for a minimum possible time (10 min) during an experiment. However, the history of melt inclusions trapped in spinels before eruption and quenching is not known. It seems likely to us that equilibration occurred between melt inclusions and host spinel in the parental magma before eruption. This assumption is consistent with the presence of euhedral crystals (Fig. 3) in the line scans of Cr-rich spinel grains. Therefore our experiments were conducted at temperature, time, fO_2 conditions that more closely resemble natural magmatic environments.

Crystallization of spinel from the melt inclusion at the crystal–liquid interface is a common post-entrapment process that may affect the observed compositions of melt inclusions [15–17]. Consistent with this view of post-entrapment crystallization, microprobe line scans near the spinel/melt inclusion boundary of an unheated grain showed compositional zoning of the spinel. Since no compositional zoning near the crystal–liquid interface of experimentally heated spinels was observed, the glasses generated during those experiments may be approaching those of the original melts. However, as shown by Gaetani and Watson [44] in their experimental investigation of melt inclusions in olivines, diffusive element exchange can also occur between the magmatic system and the trapped melt inclusion. A similar investigation for melts trapped in Cr-rich spinels would allow better estimates of original melt compositions to be made than our current understanding permits.

7.2. Source of the volcanic clastics for Tianba Formation

The presence of detrital Cr-rich spinels in sedimentary rocks of a basin within and/or adjacent to an orogenic belt is generally interpreted as an indicator of derivation from peridotites/ophiolite sequences [18–20]. Hence, the presence of significant mafic volcanic clasts and detrital Cr-rich spinels in the Tianba Formation might be assumed to be of ophiolite derivation during a Cretaceous ophiolite obduction event on the northern Indian continental margin. However, in this scenario, it would be expected that a wide variation in the chemical compositions of spinel from arc complexes would be found, because Cr-spinel from obducted ophiolite and associated subduction/accretionary materials of arc complexes have diverse origins. In contrast, the detrital spinels in the Tianba Formation have a limited range of chemical compositions, have TiO_2 content ~2%, and consistently plot in the discriminant fields of ocean island (hotspot) basalts (Fig. 4). Since the TiO_2 contents in arc spinels are generally <1%, no significant contribution of spinels from an arc-trench system to the Tianba Formation has been detected.

Clastic wedges correlative to the Tianba Formation were deposited elsewhere in the region: from the Spiti–Zanskar area, where the Giumal sandstones overlie the well-known Spiti Shale [49], to the Malla Johar and Thakkhola regions, where two >400-m-thick lithic wacke sections accumulated during a large part of the Early–mid-Cretaceous [50–53]. There are well-developed Hauterivian to Aptian sandstones in the basins of the East India coast, pointing to rejuvenation of the craton by lithospheric doming [49,54]. A large flood-basalt event (Fig. 11) linked to the activity of the Kerguelen mantle plume took place at ~117 Ma [55,56], as recorded in the Rajmahal–Sylhet–Bengal Trap Province of northeast India [57]. We suggest that this provided the volcanic clastic

Fig. 11. Paleogeography of the Tethys and surrounding continents at 117 Ma, showing the position of the Rajmahal volcanics, and the depositional sites of the mid-Cretaceous clastic sections now exposed in Zanskar and Tianba. A northward-directed subduction zone was probably located near or at the Eurasian margin. Base map from the Paleogeographic Atlas Project, University of Chicago, courtesy of David Rowley.

component to mid-Cretaceous turbiditic sandstones along the north Indian passive margin, which are now locally preserved in the Tethyan Himalayan sedimentary sections. The volcanic pile produced by the hot spot is likely to have been large, judging by the prominent trace it subsequently left of the 90E ridge, and erosion of the volcanics could have provided significant amounts of volcanic detritus, including Cr-rich spinels, for an extended time after the geologically short-lived major eruptive event.

8. Conclusion

Based both on the chemical compositions of the Cr-rich spinels and the estimated compositions of the melt inclusions in the ~5% of the spinels that contain them, the detrital Cr-rich spinels in turbiditic sandstones of the upper part of mid-Cretaceous Tianba Formation in the northern Nieru Valley, southern Tibet, were derived from mafic volcanic rocks produced in a hotspot setting. When combined with a palaeo-tectonic reconstruction for the mid-Cretaceous, these geochemical

data suggest that the Rajmahal volcanics, which were associated spatially and temporally with Kerguelen hotspot activity on India ~117 Ma ago, were the probable source for these detrital Cr-rich spinels in the Tianba Formation. Neither ophiolites nor volcanic arcs were geochemically detectable as sources of detrital components in the Tianba Formation.

References

[1] A.V. Sobolev, Melt inclusions in minerals as a source of principle petrological information, Petrology 4 (1996) 209–211.

[2] E.B. Watson, Glass inclusions as samples of early magmatic liquid: determinative method and application to a south Atlantic basalt, J. Volcanol. Geotherm. Res. 1 (1976) 73–84.

[3] P.L. Roeder, A. Poustovetov, Growth forms and composition of chromian spinel in MORB magma: diffusion-controlled crystallization of chromian spinel, Can. Mineral. 39 (2001) 397–416.

[4] A.V. Sobolev, N. Shimizu, Ultra-depleted primary melt included in an olivine from the mid-Atlantic ridge, Nature 363 (1993) 151–154.

[5] A.V. Sobolev, N. Shimizu, The origin of typical NMORB: the evidence from a melt inclusions study, Mineral. Mag. 58A (1994) 862–863.

[6] A.V. Sobolev, L.V. Danyushevsky, Petrology and geochemistry of boninites from the north termination of the Tonga trench: constraints on the generation conditions of primary high Ca boninite magmas, J. Petrol. 35 (1994) 1183–1211.

[7] A.V. Sobolev, A.W. Hofmann, I.K. Nikogosian, Recycled oceanic crust observed in 'ghost plagioclase' within the source of Mauna Loa lavas, Nature 404 (2000) 986–990.

[8] V.S. Kamenetsky, Methodology for the study of melt inclusions in Cr-spinel, and implications for parental melts of MORB from FAMOUS area, Earth Planet. Sci. Lett. 142 (1996) 479–486.

[9] L.V. Danyushevsky, F.N. Della-Pasqua, S. Sokolov, Re-equilibration of melt inclusions trapped by magnesian olivine phenocrysts from subduction-related magmas: petrological implications, Contrib. Mineral. Petrol. 138 (2000) 68–83.

[10] L.V. Danyushevsky, A.W. McNeill, A.V. Sobolev, Experimental and petrological studies of melt inclusions in phenocrysts from mantle-derived magmas: an overview of techniques, advantages and complications, Chem. Geol. 183 (2002) 4–25.

[11] V.S. Kamenetsky, S.M. Eggins, A.J. Crawford, D.H. Green, M. Gasparon, T.J. Falloon, Calcic melt inclusions in primitive olivine at 43°N MAR: evidence for melt-rock reaction/melting involving clinopyroxene-rich lithologies during MORB generation, Earth Planet. Sci. Lett. 160 (1998) 115–132.

[12] V.S. Kamenetsky, A.J. Crawford, S. Meffre, Factors controlling chemistry of magmatic spinel: an empirical study of associated olivine, Cr-spinel and melt inclusions from primitive rocks, J. Petrol. 41 (2001) 655–671.

[13] V.S. Kamenetsky, A.V. Sobolev, S.M. Eggins, A.J. Crawford, R.J. Arculus, Olivine-enriched melt inclusions in chromites from low-Ca boninites, Cape Vogel, Papua New Guinea: evidence from ultramafic primary magma, refractory mantle source and enriched components, Chem. Geol. 183 (2002) 287–303.

[14] P. Schiano, R. Clocchiatti, J.P. Lorand, D. Massare, E. Deloule, M. Chaussidon, Primitive basaltic melts included in podiform chromites from the Oman ophiolite, Earth Planet. Sci. Lett. 146 (1997) 489–497.

[15] K. Shimizu, T. Komiya, K. Hirose, N. Shimizu, S. Maruyama, Cr-spinel, an excellent micro-container for retaining primitive melts—implications for hydrous plume origin for komatiite, Earth Planet. Sci. Lett. 189 (2001) 177–188.

[16] J.-P. Lorand, G. Ceuleneer, Silicate and base metal sulfide inclusions in chromites from the Maqsad area (Oman ophiolite, Gulf of Oman): a model for entrapment, Lithos 22 (1989) 173–190.

[17] I.A. Sigurdsson, S. Steinthorsson, K. Gronvold, Calcium-rich melt inclusions in Cr-spinels from Borgarhraun, northern Iceland, Earth Planet. Sci. Lett. 183 (2000) 15–26.

[18] E. Pober, P. Faupl, The chemistry of detrital spinels and its application for the geodynamic evolution of the eastern Alps, Geol. Rundsch. 77 (1988) 641–670.

[19] H.O. Cookenboo, R.M. Bustin, K.R. Wilks, Detrital chromian spinel compositions used to reconstruct the tectonic setting of provenance: implications for orogeny in the Canadian Cordillera, J. Sediment. Res. 67 (1997) 116–123.

[20] M. Ganssloser, Detrital chromian spinels in Rhenohercynian greywackes and sandstones (Givetain-Visean, Variscides, Germany) as indicators of ultramafic source rocks, Geol. Mag. 136 (1999) 437–451.

[21] J. Dewey, M. Mange, Petrography of Ordovician and Silurian sediments in the western Irish Caledonides: tracers of short-lived Ordovician continent-arc collision orogeny and the evolution of the Laurentian Appalachian–Caledonian margin, in: C. Mac Niocaill, P.D. Ryan (Eds.), Continental tectonics, Spec. Publ.-Geol. Soc. Lond., vol. 164, 1999, pp. 55–107.

[22] D. Lenaz, V.S. Kamenetsky, A.J. Crawford, F. Princivalle, Melt inclusions in detrital spinel from SE Alps (Italy–Slovenial): a new approach to provenance studies of sedimentary basins, Contrib. Mineral. Petrol. 139 (2000) 748–758.

[23] D. Sciunnach, E. Garzanti, Sedimentary record of late Paleozoic rift and break-up in northern Gondwana (Thini Chu group and Tamba–Kurkur Fm.; Dolpo Tethys Himalaya, Nepal), Geodin. Acta 9 (1996) 41–56.

[24] A.M.C. Sengor, D. Altiner, A. Cin, T. Ustaomer, K.J. Hsu, Original assembly of the Tethyside orogenic collage at the expense of Gondwanaland, in: M.G. Audley-Charles, A. Hallame (Eds.), Gondwana and Tethys, Geol. Soc. Spec. Publ., vol. 37, 1988, pp. 119–181.

[25] E. Garzanti, Stratigraphy and sedimentary history of the Nepal Tethys Himalayan passive margin, in: B.N. Upreti, P. Le Fort (Eds.), Advances on the geology of the Himalaya—focus on Nepal, Journal of Asian Earth Sciences, vol. 17/5–6, 1999, pp. 805–827.

[26] S. Dürr, Provenance of Xigaze fore-arc basin clastic rocks (Cretaceous, South Tibet), GSA Bull. 108 (1996) 669–684.

[27] G. Einsele, B. Liu, S. Dürr, W. Frisch, G. Liu, H.P. Luterbacher, L. Ratschbacher, W. Ricken, J. Wendt, A. Wetzel, G. Yu, H. Zheng, The Xigaze forearc basin, evolution and facies architecture (Cretaceous, Tibet), Sediment. Geol. 90 (1994) 1–20.

[28] J. Burg, G. Chen, Tectonics and structural zonation of southern Tibet, China, Nature 311 (1984) 219–223.

[29] B. Zhu, W.S.F. Kidd, D.B. Rowley, B.S. Currie, Chemical compositions and tectonic significance of chrome-rich spinels in Tianba Flysch, southern Tibet, J. Geol. 112 (2004) 417–434.

[30] S. Wen, Cretaceous system, Stratigraphy of the Mount Qomolangma Region, Science Press, Beijing, 1987, pp. 160–180.

[31] Xizang BGMR (Xizang Bureau of Geology and Mineral Resources), Regional Geology of the Xizang Autonomous Region, Geological Publishing House, Beijing, 1992, 707 pp.

[32] C. Wang, X. Li, X. Wan, R. Tao, The Cretaceous in Gyangze, southern Xizang (Tibet): redefined, Acta Geol. Sin. 74 (2000) 97–107.

[33] H. Willems, Z. Zhou, B. Zhang, K.-U. Gräfe, Stratigraphy of the upper Cretaceous and lower Tertiary strata in the Tethyan Himalayas of Tibet (Tingri area, China), Geol. Rundsch. 85 (1996) 723–754.

[34] P.L. Roeder, I. Reynolds, Crystallization of chromite and chromium solubility in basaltic melts, J. Petrol. 32 (1991) 909–934.

[35] G.A. Gaetani, E.B. Watson, Open system behavior of olivine-hosted melt inclusions, Earth Planet. Sci. Lett. 183 (2000) 27–41.

[36] H.J.B. Dick, T. Bullen, Chromian spinel as a petrogenetic indicator in abyssal and alpine-type peridotites and spatially associated lavas, Contrib. Mineral. Petrol. 86 (1984) 54–76.

[37] S.J. Barnes, P. Roeder, The range of spinel compositions in terrestrial mafic and ultramafic rocks, J. Petrol. 42 (2001) 2279–2302.

[38] P.A.H. Scowen, P.L. Roeder, R.T. Helz, Reequilibration of chromite within Kilauea Iki lava lake, Hawaii, Contrib. Mineral. Petrol. 107 (1991) 8–20.

[39] J.F. Allan, R.O. Sack, R. Batiza, Cr-rich spinels as petrogenetic indicators: MORB-type lavas from the Lamont seamount chain, eastern Pacific, Am. Mineral. 73 (1988) 741–753.

[40] Y.H. Lee, Geotectonic significance of detrital chromian spinel: a review, Geosci. J. 3 (1999) 23–29.

[41] A.Y. Borisova, I.K. Nikoosian, J.S. Scoates, D. Weis, D. Damasceno, N. Shimizu, J.L.R. Touret, Melt, fluid and crystal inclusions in olivine phenocrysts from Kerguelen plume-derived picritic basalts: evidence for interaction with Kerguelen Plateau lithosphere, Chem. Geol. 183 (2002) 195–220.

[42] M.J. Le Bas, R.W. Le Maitre, A. Streckeisen, B. Zanettin, A chemical classification of volcanic rocks based on the total alkali–silica diagram, J. Petrol. 27 (1986) 745–750.

[43] Geochemistry of Rocks of the Oceans and Continents. http://georoc.mpch-mainz.gwdg.de.

[44] G.A. Gaetani, E.B. Watson, Modeling the major-element evolution of olivine-hosted melt inclusions, Chem. Geol. 183 (2002) 25–41.

[45] Basaltic Volcanism Study Project, Basaltic Volcanism on the Terrestrial Planets, Pergamon Press, Inc., New York, 1981, 1286 pp.

[46] J. Aitchison, The Statistical Analysis of Composition Data, Chapman and Hall, New York, NY, 1986, 416 pp.

[47] R. Kent, A.D. Saunders, P.D. Kempton, N.C. Ghose, Rajmahal basalts, eastern India: mantle sources and melt distribution at a volcanic rifted margin, in: J.J. Mahoney, M.F. Coffin (Eds.), Large Igneous Provinces: Continental, Oceanic, and Planetary Flood Volcanism, 1997, pp. 145–182.

[48] M. Storey, R.W. Kent, A.D. Saunders, V.J.M. Salters, J.M. Hergt, H. Whitechurch, J.H. Sevigny, M.F. Thirlwall, P.T. Leat, N.C. Ghose, M.G. Gifford, Lower Cretaceous volcanic rocks along continental margins and their relationship to the Kerguelen Plateau, Proc. Ocean Drill. Prog., Sci. Results 120 (1992) 33–54.

[49] E. Garzanti, Sedimentary evolution and drowning of a passive margin shelf (Giumal Group; Zanskar Tethys Himalaya, India): palaeoenvironmental changes during final break-up of Gondwanaland, in: P. Treloar, M. Searle (Eds.), Himalayan Tectonics, Special Publication-Geological Society of London, vol. 74, 1993, pp. 277–298.

[50] A. Sinha, Geology of the Higher Central Himalaya, John Wiley & Sons, New York, 1988, 219 pp.

[51] S. Dürr, M.R. Gibling, Early Cretaceous volcaniclastic and quartzose sandstones from north central Nepal: composition, sedimentology and geotectonic significance, Geol. Rundsch. 83 (1994) 62–75.

[52] M.R. Gibling, F.M. Gradstein, I.L. Kristiansen, J. Nagy, M. Sarti, J. Wiedmann, Early Cretaceous strata of the Nepal Himalayas: conjugate margins and rift volcanism during Gondwanan breakup, J. Geol. Soc. 151 (1994) 269–290.

[53] F. Jadoul, F. Berra, E. Garzanti, The Tethys Himalayan passive margin from late Triassic to Early Cretaceous (South Tibet), J. Asian Earth Sci. 16 (1998) 173–194.

[54] I. Campbell, R. Griffiths, Implications of mantle plume structure for the evolution of flood basalts, Earth Planet. Sci. Lett. 99 (1990) 79–93.

[55] A. Baksi, Petrogenesis and timing of volcanism in the Rajmahal flood basalt province, NE India, Chem. Geol. 121 (1995) 73–90.

[56] R.W. Kent, M.S. Pringle, R.D. Muller, A.D. Saunders, N.C. Ghose, 40Ar/39Ar geochronology of the Rajmahal Basalts, India, and their relationship to the Kerguelen Plateau, J. Petrol. 43 (2002) 1141–1153.

[57] S. Ingle, D. Weis, J.S. Scoates, F.A. Frey, Relationship between the early Kerguelen plume and continental flood basalts of the paleo-Eastern Gondwanan margins, Earth Planet. Sci. Lett. 197 (2002) 35–50.